Atmos. Chem. Phys. Discuss., 6, 12155–12178, 2006
www.atmos-chem-phys-discuss.net/6/12155/2006/

Atmospheric Chemistry and Physics Discussions

SAWA experiment – properties of mineral dust aerosol as seen by synergic lidar and sun-photometer measurements

A. E. Kardas[1], K. M. Markowicz[1], S. P. Malinowski[1], G. Karasiński[2], T. Stacewicz[2], K. Stelmaszczyk[3], C. Hochhertz[3], and L. Woeste[3]

[1]Institute of Geophysics, Warsaw University, Poland
[2]Institute of Experimental Physics, Warsaw University, Poland
[3]Free University of Berlin, Germany

Received: 28 September 2006 – Accepted: 20 November 2006 – Published: 28 November 2006

Correspondence to: A. E. Kardas (aekardas@igf.fuw.edu.pl)

Abstract

We propose a method of retrieving basic information on mineral dust aerosol particles from synergic sun-photometer and multi-wavelength lidar measurements as well as from the observations of lidar light depolarisation. We use this method in a case study of mineral dust episode in Central Europe.

Lidar signals are inversed with a modified Klett-Fernald algorithm. Aerosol optical depth measured with the sun-photometer allows to reduce uncertainties in the inversion procedure through which we estimate vertical profile of aerosol extinction.

Next we assume that aerosol particles may be represented by ensemble of randomly oriented, identical spheroids. Having calculated vertical profiles of aerosol extinction coefficients for lidar wavelengths, we compute the profiles of local Angstrom exponent. We use laser beam depolarisation together with the calculated Angstrom exponents to estimate the shapes (aspect ratios) and sizes of the spheroids. Numerical calculations are performed with the transition matrix (T-matrix) algorithm by M. Mishchenko.

The proposed method was first used during SAWA measurement campaign in Warsaw, spring 2005, to characterise the particles of desert dust, drifting over Poland with a southern-eastern wind (13–14 April). Observations and T-matrix calculations show that mode radii of spheroids representative for desert aerosols' particles are in the range of 0.15–0.3 μm, while their aspect ratios are lower than 0.7 or larger than 1.7.

1 Introduction

It is now commonly known, that aerosols' role in the global climate and its change is important and complex (Houghton, 2001; Satheesh and Krishna Moorthy, 2005). In case of many aerosol types it is not yet established, whether their net contribution to the Earth surface heat balance is positive or negative (Shine and de F. Forster, 1999). One of them is mineral dust (Sokolik and Toon, 1996) emitted from the Earth surface in desert areas and often transported in the atmosphere at long distances. Typical source

areas of dust events observed in Europe are Sahara and Arabian deserts. In this paper we describe investigation of the optical properties of mineral dust transported in the middle atmosphere from these source regions to Poland. Such events are common in Central Europe during the spring time (Borbély-Kiss et al., 2004). We analyse a particular episode of 13–14 April 2005, when a dust plume drifted over Warsaw carried by flow from south and south east. Observations and measurements we describe were performed during SAWA campaign held in spring 2005 at emerging aerosol/radiative transfer laboratory of Warsaw University.

As the campaign was focused on dust events, in order to plan the intensive measurement periods, a long range NAAPS (Navy Aerosol Analysis and Prediction System) was used as a forecast tool. Prediction of a dust plume investigated in this study is presented in Fig. 1.

Among many radiometric instruments used during the campaign were sun-photometers (Microtops and a prototype multi-spectral device Markowicz and Kardas, 2006) and the aerosol lidar (Teramobile Profiler from the Free University of Berlin). Microtops measures direct solar radiation in five channels between 380 and 870 nm. Its built-in algorithm produces total Aerosol Optical Depth (AOD) in each channel.

Teramobile Profiler is a multi-wavelength backscattering lidar, originally developed for delivering atmospheric parameters (particle and aerosol density profiles) during experiments on non-linear propagation of ultra-short femtosecond laser pulses in the atmosphere (Rodriguez et al., 2004; Mechain et al., 2005). It is based on a solid-state 10 Hz Nd:Yag laser (Big Sky Laser CFR 200), which delivers 10 ns long pulses of energies of 60, 50, 30 and mJ, in 1064 nm, 532 nm and 355 nm wavelengths, respectively. As a receiver the lidar uses F4/200 mm Newtonian telescope. Optical system has a multi-axial design, in which each wavelength is emitted as a separate beam in the vertical direction. The inclination of each beam can be individually adjusted assuring fairly equal overlap with telescope's field-of-view, which compensates the geometrical compression effect (Stelmaszczyk et al., 2005). The backscattered light collected by the telescope is spectrally separated. Its intensity is measured independently at each

wavelength with the photo-multipliers (Hammamatsu R7400 -P04 and -U02 for 355 nm and 532 nm) and with the avalanche photo-diode (EG&G C30954/5E for 1064 nm). All signals are recorded with a 12-bit, 20 MHz transient recorder (Licel) assuring vertical spatial resolution of 7.5 m. Data are then averaged, typically over 1000 laser shots (~1 min). Intensity of the 532 nm signal is measured in two polarisations, in directions parallel and perpendicular to the polarisation of the emitted signal. Usually depolarisation of the returned signal is an indicator of non–sphericity of scattering objects, which may help in the evaluation of radiative properties of irregular mineral dust.

In this study we analyse data collected with use of Microtops and Teramobile Profiler taking a special concern in synergy of the measurements. The main idea is to use information on the aerosol optical depth obtained from passive photometer in order to reduce the number of assumptions necessary to invert the lidar signal. Then, with an additional assumption that the particles may be represented by ensemble of randomly oriented, identical spheroids, the size and aspect ratio of the observed aerosol particles are estimated. This assumption allows to adopt the Transition matrix (T-matrix) algorithm by Mishchenko and Travis (1998), in order to calculate scattering properties of the dust.

The paper is organized in the following manner. In the next section details of data processing algorithms and procedures are described. In Sect. 3 results of the measurements are presented and discussed. A short summary and conclusions are given in the last section of the article.

2 Data processing

2.1 Lidar signal inversion method

The idealised lidar equation can be written after Klett (1981) and Fernald (1984):

$$S(z) = \frac{CE}{z^2}[\beta_R(z) + \beta_A(z)]T_R^2 T_A^2. \quad (1)$$

Here S is the ideal lidar signal, z is the distance from the lidar (in this case simply height), C – the lidar constant, E – the laser impulse energy, β_R and β_A – backscatter coefficients for molecules and aerosol particles, T_R and T_A – the molecular and aerosol trasmittances.

Solving Eq. (1) requires introducing a new variable:

$$P(z) = \frac{S(z)}{E} z^2, \tag{2}$$

and assuming a relationship between aerosol's backscatter and extinction coefficient (a_A) (Fernald, 1984):

$$\beta_A(z) = R_A(z) a_A(z). \tag{3}$$

The R_A coefficient is called the lidar ratio.

Equation (3) allows to calculate the unknown value of the aerosol transmittance in Eq. (1), as:

$$T_A = \exp\left(-\int a(z)dz\right) = \exp\left(-\int \frac{\beta_A(z)}{R_A(z)} dz\right). \tag{4}$$

In order to estimate this integral usually a simplifying assumption that R_A is independent of z is adopted (Landulfo et al., 2003; Iwasaka et al., 2003; Welton et al., 2000). Then the solution of Eq. (1) may be written in the following form:

$$\beta_A(z) = \frac{P(z) T_R^{2(r-1)}(z)}{C - \frac{2}{R_A}\int_0^z P(z') T_R^{2(r-1)}(z') dz'} - \beta_R(z), \tag{5}$$

where

$$r = \frac{R_R}{R_A} \tag{6}$$

and R_R=3/8π is the backscatter to extinction ratio in Rayleigh scattering.

Calculations with the modified Klett-Fernald algorithm begin at the top of the measurement range, assuming $\beta_A(z_{max})$=0 . Then pairs of equations similar to Eq. (5), written for subsequent levels in the atmosphere, *"z"* and *"z-dz"* are solved. This allows to avoid the necessity of establishing the value of the lidar constant C (Welton et al., 2000). $\beta_R(z)$ is usually calculated with empirical equations for assumed or measured vertical profiles of temperature and pressure in the atmosphere.

Nevertheless there is still one unknown remaining: R_A. In order to evaluate it we propose the following iterative procedure. In the first step we assume R_A=1 or R_A=R_R. Then, after calculating the whole vertical profile of β_A , R_A is redefined as:

$$R_A = \frac{\int \beta_A(z) dz}{\tau_{SP}}, \tag{7}$$

where τ_{SP} is the total optical depth of aerosol, measured with the sun-photometer (Welton et al., 2000). The calculations begin again at the top of the range and the procedure is repeated until the difference between subsequent values of R_A is sufficiently small. With this additional bond the common practise (Landulfo et al., 2003; Iwasaka et al., 2003) of guessing R_A's value is avoided.

The next improvement of the procedure comes from the following observation. When several aerosol layers are present in the atmosphere, it is advisable to allow for R_A to differ between them. Therefore it is desirable to divide the atmosphere into appropriate layers determined on the basis of the lidar backscatter signal. More details on the particular division adopted in the case study can be found in Sect. 3.2. Here we briefly describe the way, in which the improvement can be adopted. In first step extinction coefficient profiles should be calculated for the whole atmosphere. Then, integration within the chosen height ranges should give optical depth values to be used instead τ_{SP} while running the algorithm for each layer separately.

2.2 Numerical calculations (T-matrix)

One of the goals of the SAWA campaign was to find a mathematical representation of the dust particles, suitable for a radiative transfer model. This required the possibility of evaluating the properties of particles on the basis of measured values. We decided to use the transition matrix (T-matrix) method, initially developed by Waterman (1971) and implemented by Mishchenko and Travis (1998), consisting basically on the numerical solution of Maxwell's equations.

Electric field of the incident (E^i) and scattered by a single particle radiation (E^s) is expanded in vector spherical functions M_{mn} and N_{mn} (Tsang et al., 1985):

$$E^i(\boldsymbol{R}) = \sum_{n=1}^{n_{\max}} \sum_{m=-n}^{n} [a_{mn}\boldsymbol{R}gM_{mn}(\boldsymbol{R}) + b_{mn}\boldsymbol{R}gN_{mn}(\boldsymbol{R})] \tag{8}$$

$$E^s(\boldsymbol{R}) = \sum_{n=1}^{n_{\max}} \sum_{m=-n}^{n} [p_{mn}M_{mn}(\boldsymbol{R}) + q_{mn}N_{mn}(\boldsymbol{R})] \,. \tag{9}$$

Here the origin of the coordinate system is assumed to be inside the particle, $\boldsymbol{R}$ is the vector of position (larger than the radius of a scattering particle's circumscribing sphere), g – the asymmetry parameter, a_{mn}, b_{mn} , p_{mn} and q_{mn} – coefficients.

As the Maxwell's equations and boundary conditions are linear, the relationship between coefficients for scattered and incident light may be represented by a transition matrix (**T**) (Mishchenko and Travis, 1998):

$$[p, q] = \mathbf{T}[a, b]. \tag{10}$$

The elements of a T-matrix depend only on the physical characteristics of the particle, such as size, shape, refractive index and orientation. Therefore once calculated, a T-matrix can be used in computations for any directions of beam incidence or scattering. Furthermore this approach is also useful in modelling the interaction between light and an ensemble of randomly oriented particles.

The standard procedure for calculating the transition matrix for a non-spherical particle uses the extension of the particle's internal filed extended in vector spherical functions analogically to Eqs. (8) and (9) (Waterman, 1971). The T-matrix may be calculated for particles of arbitrary shapes, but the formulas simplify decidedly, while a rotational symmetry is assumed.

We assume that the observed dust particles can be represented by an ensemble of randomly oriented spheroids with a log-normal size distribution and fixed aspect ratios. This allows us to create look-up tables for evaluating particles' parameters on the basis of the lidar and the sun-photometer retrievals (Sects. 2.3 and 2.4).

The necessary numerical calculations were performed with the use of the T-matrix FORTRAN routine (Mishchenko and Travis, 1998) available on http://www.giss.nasa.gov/~crmim/t_matrix.html.

2.3 Determination of particles' size

We decided to estimate the mean size of the particles, using the values of the Angstrom exponent (α), retrieved from the profiles of extinction coefficient at different wavelengths. T- matrix code was used to perform numerical simulations of the light transfer through an ensemble of particles mentioned in Sect. 2.2. 532 nm wavelength and the refractive index of sand, equal to 1.53+0.008i were assumed.

Results of calculations for a number of different mode radii show, that at least within a limited particle radius range (0.1–0.6 μm), the relationship between α and the mean radius is monotonic and shape-independent. This can be observed in Fig. 2, where the plots corresponding to different spheroids' aspect ratios overlap. Aspect ratio 2 means oblate spheroids, 0.5 – prolate, 1 – spheres.

Reading Fig. 2 is useful in order to estimate the mode radius of spheroids representative for observed particles.

2.4 Determination of particles' shape

A parameter which is highly sensible to particles' shape is the depolarisation of the returning lidar signal, defined as:

$$\delta = P_R / P_L . \tag{11}$$

Here P_R and P_L are the values of lidar returns with polarisations perpendicular and parallel to the polarisation of the original beam (Stephens, 1994).

T-matrix simulations performed for different mode radii of aerosol particles (Fig. 3) show, that δ can be used in estimating the aspect ratio of aerosol particles for single scattering approach, as it always equals zero for spheres and is decidedly higher for spheroids. Unfortunately the result is not unequivocal – there are at least two possible aspect ratios for given size and each non-zero depolarisation.

3 Experimental results

3.1 SAWA measurement campaign

As mentioned, SAWA experiment took place in April and May 2005, in Warsaw. Its main goal was to examine the aerosols typical for the desert dust episodes in Central Europe. During the campaign one major event of this kind appeared, between 12 and 19 April. Synergic lidar and sun-photometer measurements were made on 13 and 14 April. Unfortunately, as it was noticed later, the UV channel of the Teramobile Profiler was not operating correctly and its records were not accounted in the analysis.

Figure 4 presents lidar returns in wavelength 532 nm, collected on 13 and 14 April. In the atmospheric boundary layer between the surface and the level of approximately 1.5 km one may observe large concentrations of presumably urban aerosols (strong lidar signals). Higher, up to 4–5 km, the relatively wide layer of increased returns, likely due to the enhanced aerosol concentration, is clearly visible (grey). Its presence is

in agreement with the prediction of NAAPS model presented in Fig. 1, which shows a dust plume transported in the middle troposphere from the regions of Sahara and Arabian Desert.

3.2 Measured AODs and aerosol extinction profiles

During SAWA experiment total aerosol optical depths were measured with Microtops sun-photometer. As the instrument measures direct solar radiation, it can only be used during day time and when the sun's disc is not obscured by clouds. This means, that there are gaps in the Microtops measurement series, especially during the night time. In these gaps values of AOD were linearly interpolated between measurement times.

AODs measured during the dust episode (Fig. 5) were noticeably higher than those observed on other days. For example on the 14 April (Fig. 5b) the optical depth in 500 nm wavelength reached 0.67 in contrast to values of 0.05–0.25 characteristic for days without the drifting dust in the middle troposphere.

Since Microtops channels do not agree with the lidar ones, in order to estimate AODs in the lidar wavelengths Microtops measurements had to be transformed with the use of the Angstrom power law (Angstrom, 1964). In the adopted procedure atmosphere was divided into three layers: boundary layer (urban aerosols), desert dust and "clear" air (Fig. 6). The first border discriminating between the boundary layer and the desert dust layer in the troposphere was assumed between 1 and 1.5 km heights, at the level of the local minimum of the lidar return signal. The upper border of the mineral aerosol layer was set between 4.95 km and 5.6 km, at the level of minimum depolarisation of the lidar signal (Fig. 7).

Estimates based on the preliminary application of Klett algorithm (considering atmosphere as a single layer) show that the optical thickness of mineral dust was comparable to that of the boundary layer aerosol – see Fig. 8. When consulting the figure notice, that in the night time, when we did not have reliable measurements of AODs and linear interpolation of Microtops measurements filled the gap in the data, the adopted procedure is less reliable than during the day.

From the lidar signals at 532 and 1064 nm profiles of extinction coefficients were derived, following the procedure described in Sect. 2.2. Figure 9 shows result for 532 nm wavelength. Extinction coefficients in the desert dust layer are in the range of $0.5\times10^{-4}\,m^{-1}$ to $1.5\times10^{-4}\,m^{-1}$. They are lower than the values observed for the urban aerosols, but as the dust layer is relatively thick its influence on radiative flux is important.

3.3 Estimations of particles' sizes and shapes

Figure 10 shows vertical profiles of the local Angstrom exponent computed from the extinction coefficients for 532 nm and 1064 nm wavelengths. Values in the lowest layer (consult Fig. 6) are between 0.5 and 1.5, which corresponds to the particles of radii in the range 0.25–0.35 μm (see Fig. 2). In the middle layer (with the desert dust aerosol), Angstrom exponents are in the range of 0.7–2.5, which corresponds to the particles of radii in the range 0.15–0.3 μm.

Figure 7, already mentioned in Sect. 3.2, presents signal depolarisation calculated for the 532 nm wavelength. Comparing the depolarisation in the lowest layer and in the middle layer with desert aerosol we see, that mineral dust of depolarisation larger than 0.1 differs decidedly from the aerosol in the boundary layer whose depolarisation is close to zero. As Fig. 3 indicates, such level of depolarisation means that the aspect ratios of spheroids representative for mineral dust are more than 1.7 in the case of oblate spheroids or less than 0.7 in the case of prolate spheroids.

4 Conclusions

A dust episode observed on 13 and 14 April 2005 during SAWA campaign held in Warsaw is analysed. Synergic measurements by the means of multi-wavelength lidar and Microtops sun-photometer allow to reduce the number of assumptions needed to retrieve profiles of extinction coefficients. These profiles together with an additional

information on the depolarisation of the lidar signal and assumption of the spheroidal shape of aerosol particles, were used in numerical calculations performed using the T-matrix code. As the result we estimated sizes and shapes (aspect ratios) of the observed mineral dust particles.

The mode radii of these particles is in the range of 0.15–0.3 μm. This is consistent with the values commonly used in modelling radiative processes for aerosol type "mineral transported" (Hess et al., 1998). The aspect ratios of spheroids representative for the observed mineral dust are smaller than 0.7 or larger than 1.7. This result is important, since recent studies indicate that non-sphericity of the particles may cause up to 10% positive or negative change in the aerosol forcing (Markowicz et al., 2005).

The retrieved information of the size and shape of the mineral dust particles transported on the long distances from Sahara and Arabian deserts will be used in the new radiative model of dust.

Acknowledgements. This research was supported by 2 P04D 06927 research grant from Polish Ministry of Education and Science. Some activities related to this research were supported by the European Commission Fifth Framework Program's Project EVK2-CT2002-80010-CESSAR. We thank to all graduate students, in particular to M. Witek and M. Posyniak for their help with the SAWA measurement campaign.

References

Angstrom, A.: The parameters of atmospheric turbidity, Tellus, 16, 64–75, 1964. 12164

Borbély-Kiss, I., Kiss, Á.Z., Koltay, E., Szabó, G., and Bozó, L.: Saharan dust episodes in Hungarian aerosol: Elemental signatures and transport trajectories, J. Aerosol Sci., 35, 1205–1224, 2004. 12157

Fernald, F. G.: Analysis of atmospheric lidar observations: some comments, Appl. Opt., 23, 652–653, 1984. 12158, 12159

Hess, M., Kopepke, P., and Schult, I.: Optical Properties of Aerosol and Clouds: The Software Package OPAC, Bull. Am. Meteorol. Soc., 79, 831–844, 1998. 12166

Houghton, J. T.: Climate change 2001: the scientific basis: contribution of Working Group I to the third asessement report of the Intergovernemental Panel on Climate Change, Cambridge University Press, Cambridge, UK, New York, 2001. 12156

Iwasaka, Y., Shibata, T., Nagatani, T., Shi, G.-Y., Kim, Y. S., Matsuki, A., Trochkine, D., Zhang, D., Yamada, M., Nagatani, M., Nakata, H., Shen, Z., Li, G., Chen, B., and Kawahira, K.: Large depolarization ratio of free tropospheric aerosols over the Taklamakan Desert revealed by lidar measurements: Possible diffusion and transport of dust particles, J. Geophys. Res., 108, ACE 20-1–8, 2003. 12159, 12160

Klett, J. D.: Stable analytical inversion solution for processing lidar returns, Appl. Opt., 20, 211–220, 1981. 12158

Landulfo, E., Papayannis, A., Artaxo, P., Castanho, A. D. A., De Freitas, A. Z., Souza, R. F., Vieira Junior, N. D., Jorge, M. P., Sanchez-Ccoyllo, O. R., and Moreira, D. S.: Synergetic measurements of aerosol over Sao Paulo, Brazil, using LIDAR, sunphotometer and satellite data during the dry season, Atmos. Chem. Phys., 3, 1523–1539, 2003. 12159, 12160

Markowicz, K.M., Kardas, A.E., Hochherz, C., Stelmaszczyk, K., Rozwadowska, A., Zielinski, T., Karasinski, G., Remiszewska, J., Witek, M., Malinowski, S. P., Stacewicz, T., and Woeste, L.: Observation of aerosol properties and radiative forcing of nonspherical particles over Poland, ACCENT symposium, Urbino, 2005. 12166

Markowicz, K. M. and Kardas, A. E.: Retrieval of aerosol optical properties and estimation of aerosol forcing based on multi-spectral sun-photometer observations. 12th Conference on Cloud Physics (Madison, WI, USA, 09–14 July 2006), available at http://ams.confex.com, 2006. 12157

Mechain, G., Mejean, G., Ackermann, R., Rohwetter, P., Andre, Y.-B., Kasparian, J., Prade, B., Stelmaszczyk, K., Yu, J., Salmon, E., Winn, W., Schlie, L. A., Mysyrowicz, A., Sauerbrey, R., Woeste, L., and Wolf, J.-P.: Propagation of fs TW laser filaments in adverse atmospheric conditions, Appl. Phys. B, 80, 785–789, 2005. 12157

Mishchenko, M. I. and Travis, L. D.: Capabilities and limitations of a current FORTRAN implementation of the T-matrix method for randomly oriented rotationally symmetric scatterers, J. Quant. Spectrosc. Radiat. Transfer, 60, 309–324, 1998. 12158, 12161, 12162

Rodriguez, M., Bourayou, R., Mejean, G., Kasparian, J., Yu, J., Salmon, E., Scholz, A., Stecklum, B., Eisloffel, J., Laux, U., Hatzes, A. P., Sauerbrey, R., Woeste, L., and Wolf, J.-P.: Kilometer-range non-linear propagation of femtosecond laser pulses, Phys. REV. E, 69, 036607-1–036607-7, 2004. 12157

Satheesh, S. K. and Krishna Moorthy, K.: Radiative effects of natural aerosols: a review, Atmos. Environ., 39, 2089–2110, 2005. 12156

Shine, K. P. and Forster, P. M. D. F.: The effect of human activity on radiative forcing of climate change: a review of recent developments, Glob. Planet. Change, 20, 205–225, 1999. 12156

Sokolik, I. N. and Toon, O. B.: Direct radiative forcing by airborne mineral aerosols, J. Aerosol Sci., 27, S11–S12, 1996. 12156

Stelmaszczyk, K., Dell'Aglio, M., Chudzynski, S., Stacewicz T., and Woeste, L.: Analytical function for lidar geometrical compression form-factor calculations, Appl. Opt., 44, 1323–1331, 2005. 12157

Stephens, D. L.: Remote Sensing of the Lower Atmosphere, University Press, New York, 1994. 12163

Tsang, L., Kong, J. A., and Shin, T. Y.: Theory of Microwave Remote Sensing, Wiley, New York, 1985. 12161

Waterman, P. C.: Symmetry, Unitarity, and Geometry in Electromagnetic Scattering, Phys. Rev. D., 3, 825–839, 1971. 12161, 12162

Welton, E. J., Voss, K. J., Gordon, H. R., Maring, H., Smirnov, A., Holben, B., Schmidt, B., Livingston, J. M., Russel, P. B., Durkee, P. A., Formenti, P., and Andreae, M. O.: Ground-based lidar measurements of aerosols during ACE-2: instrument description, results and comparisons with other ground-based and airborne measurements, Tellus, 52B, 636–651, 2000. 12159, 12160

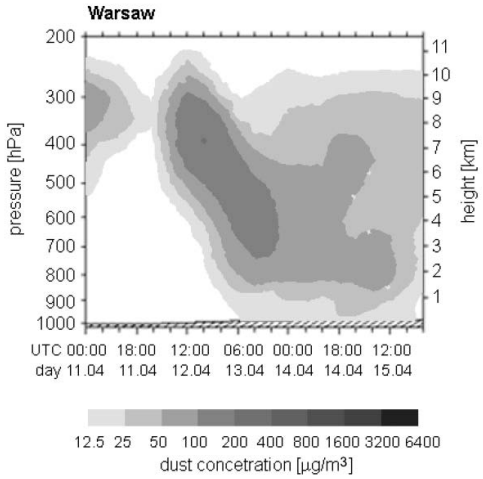

Fig. 1. Dust concentration forecast over Warsaw taken from the NAAPS model, NRL Monterey Aerosol Page (http://www.nrlmry.navy.mil/aerosol/). The largest concentrations of dust were forecasted on 12–13 April 2005, above 3 km level.

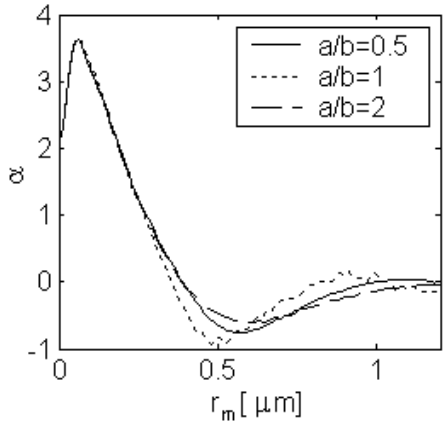

Fig. 2. Angstrom exponent's (α) dependency of the mode radius (r_m) of randomly oriented spheroids with a log-normal size distribution, calculated for the refractive index of sand and various aspect ratios (a/b). In the radii range of 0.1–0.6 μm, the relationship between α and the mean radius is monotonic and shape-independent.

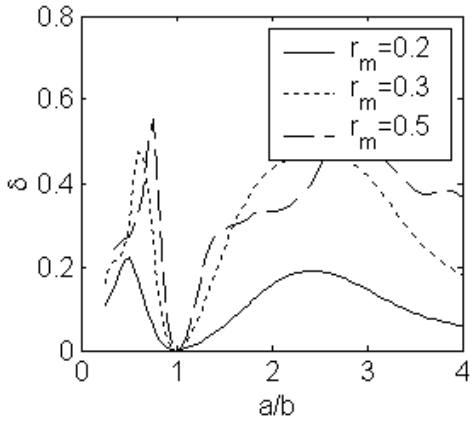

Fig. 3. Depolarisation's (δ) dependency of the aspect ratio (a/b) of randomly oriented spheroids with a log-normal size distribution, calculated for the refractive index of sand and different mode radii ($r_m[\mu m]$). The value always reaches 0 for spherical particles (a/b=1).

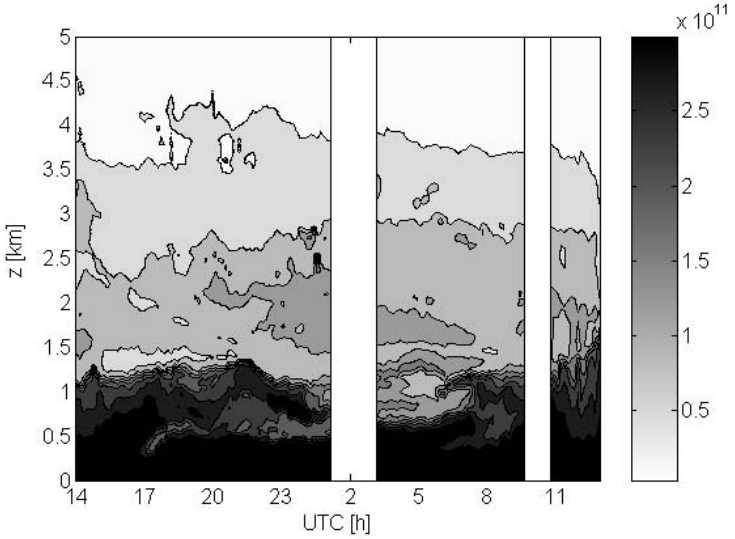

Fig. 4. Temporal evolution of lidar returns recorded for 532 nm wavelength on 13–14 April 2005 in Warsaw (arbitrary units). Light and moderate grey areas located between 1.2 and 4 km correspond to the mineral dust layer.

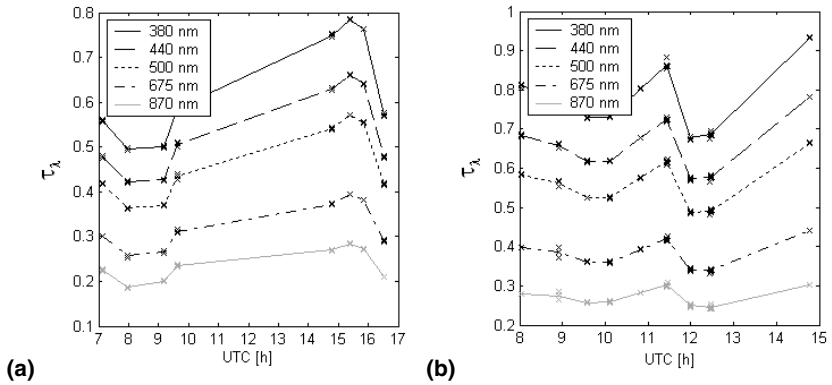

Fig. 5. Temporal evolution of aerosol optical depth (AOD) measured with Microtops on the 13 **(a)** and 14 **(b)** April 2005 in Warsaw.

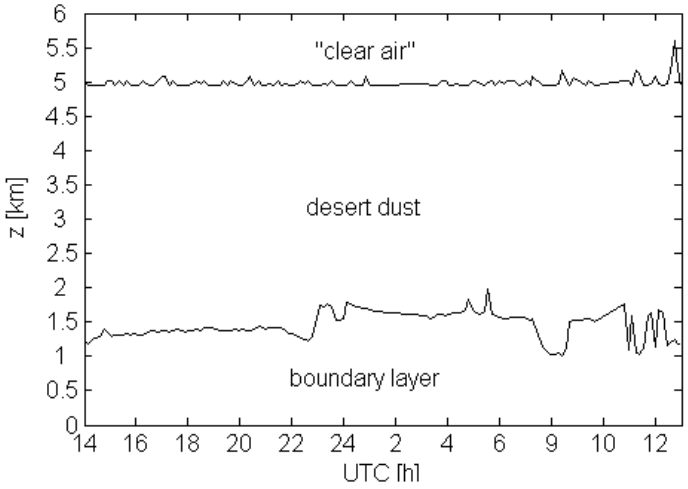

Fig. 6. Assumed division of atmosphere into three different layers – the boundary layer, the desert dust layer and the clear air layer.

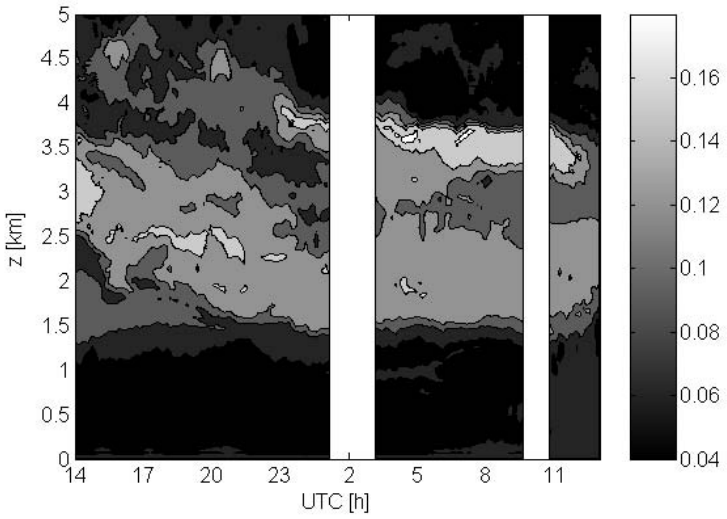

Fig. 7. Temporal evolution of light depolarisation profile measured by lidar at 532 nm wavelength, 13–14 April 2005, Warsaw. Relatively high depolarisation values (grey layer between 1.2 and 4 km) correspond to mineral dust.

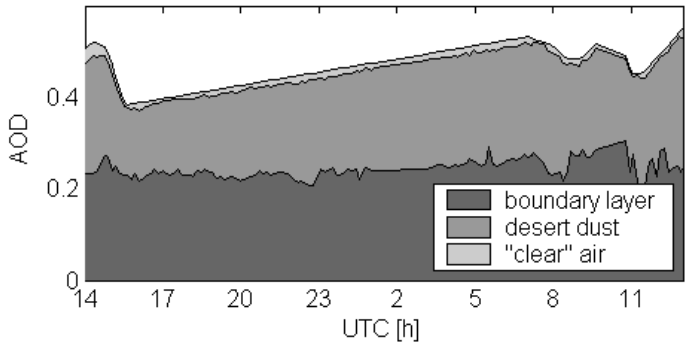

Fig. 8. Temporal evolution of aerosol optical depths (AOD) of atmospheric layers estimated on the basis of Microtops and lidar measurements on the 13–14 April 2005 in Warsaw (532 nm wavelength). Total AODs are linearly interpolated between measurement times.

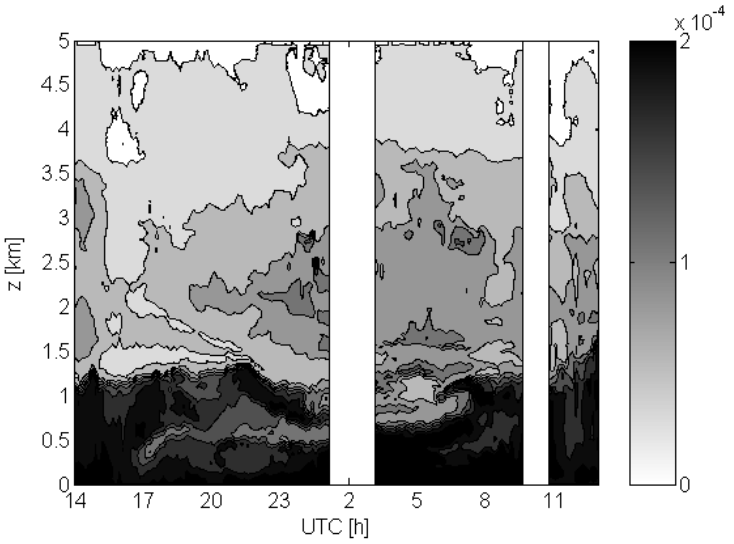

Fig. 9. Temporal evolution of aerosol extinction coefficient [1/m] vertical profiles retrieved from lidar returns for the wavelength 532 nm on 13–14 April 2005.

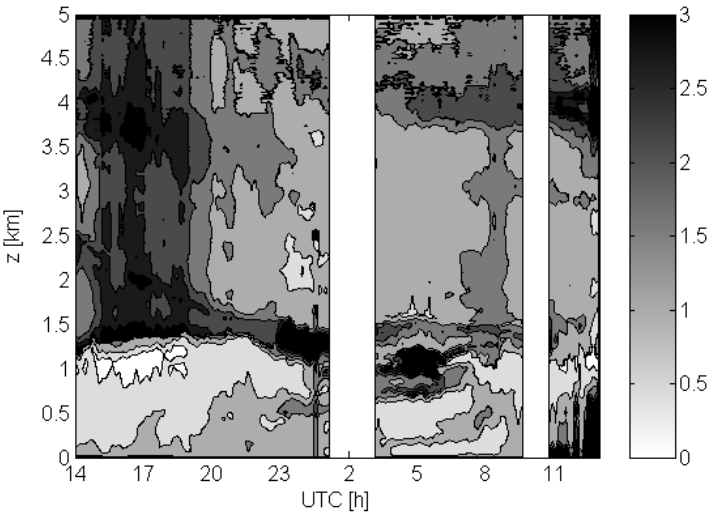

Fig. 10. Temporal evolution of Angstrom exponent vertical profiles calculated on the basis of aerosol extinctions coefficients for 532 and 1064 nm wavelengths, on the 13–14 April 2005.